CHAPTER 3

MATERIALS AND METHODOLOGY

3.1 General

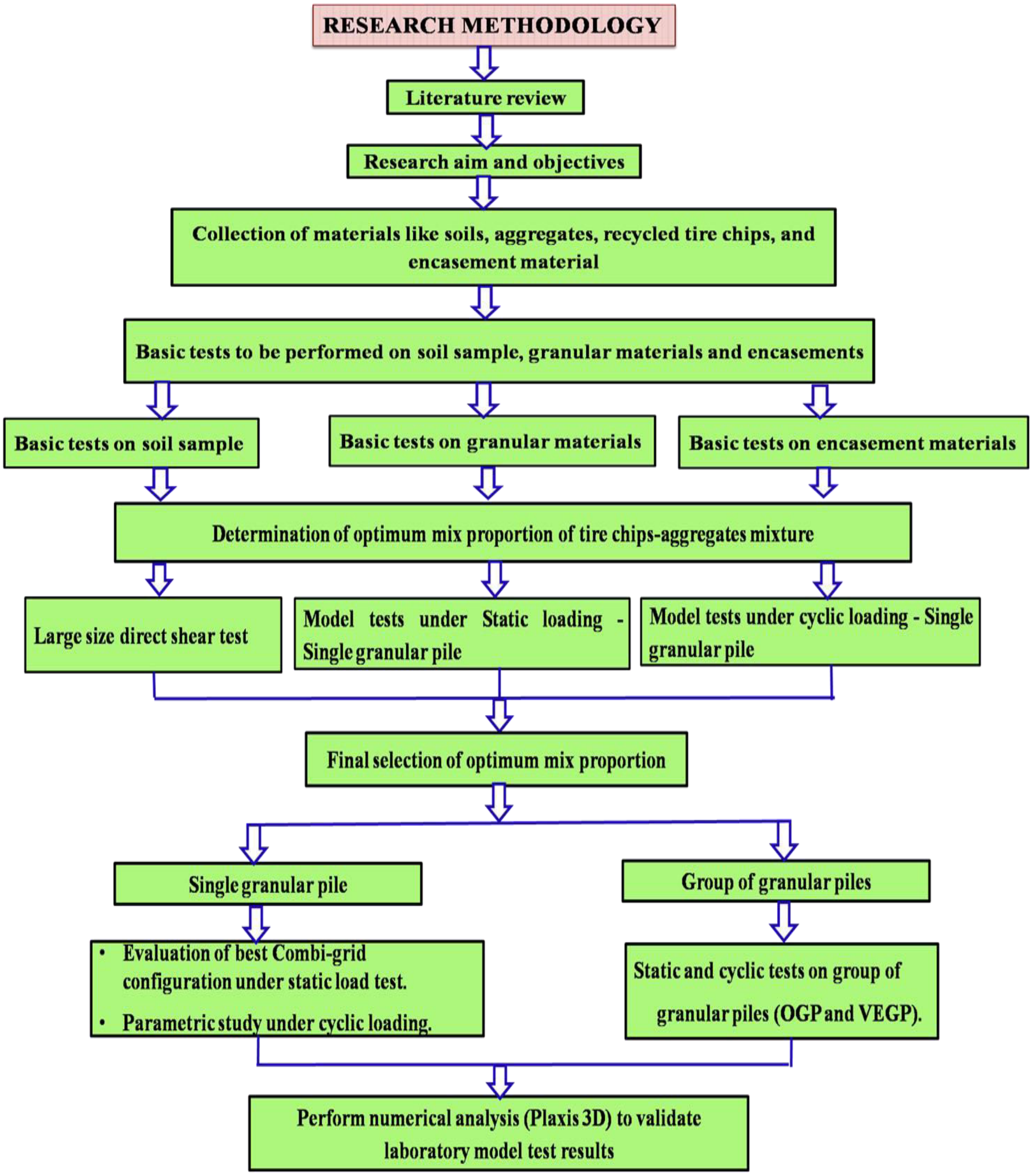

Fig. 3.1 Research methodology in a nutshell.

3.2 Test materials

This study used four basic materials: silty soil, aggregates, recycled tire chips from ELTs, and sand. These materials have the following properties.

3.2.1 Silty soil

The soft soil bed is prepared in all model studies using silty soil presented in Fig. 3.2(a). The silty soil utilized in model tests was procured from various boreholes at depths of about 2.5 to 3 m after removing vegetation near Kaithi village, Hamirpur district, Uttar Pradesh, India. These soil extracts were packed in plastic bags and brought to the laboratory without losing natural moisture content. All basic experiments, including grain size distribution, were performed on the soil as per relevant Indian standards. The basic properties of the soft soil employed in this investigation are presented in Table 3.1.

Fig. 3.2(a) Silty soil used in the study.

The grain size distribution curve of the soil sample is represented in Fig. 3.2(b). The grain size distribution curve results showed that the silt fraction is 72%, the clay fraction is 13%, the sand fraction is 10%, the gravel fraction is 5%, and the soil is classified as ML, corresponding to the unified soil classification system (USCS).

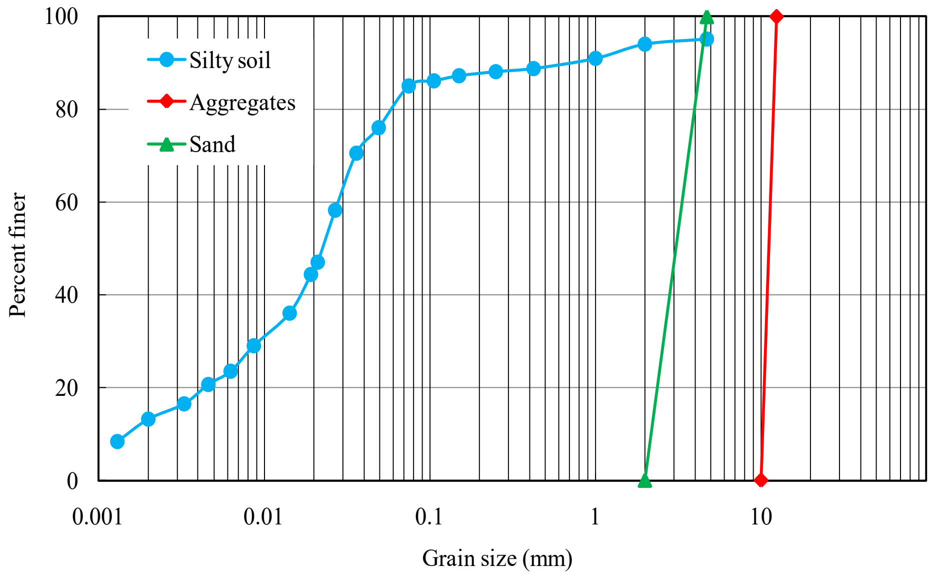

`**Fig. 3.2(b)** Grain size distribution curve for silty soil, sand, and aggregates.

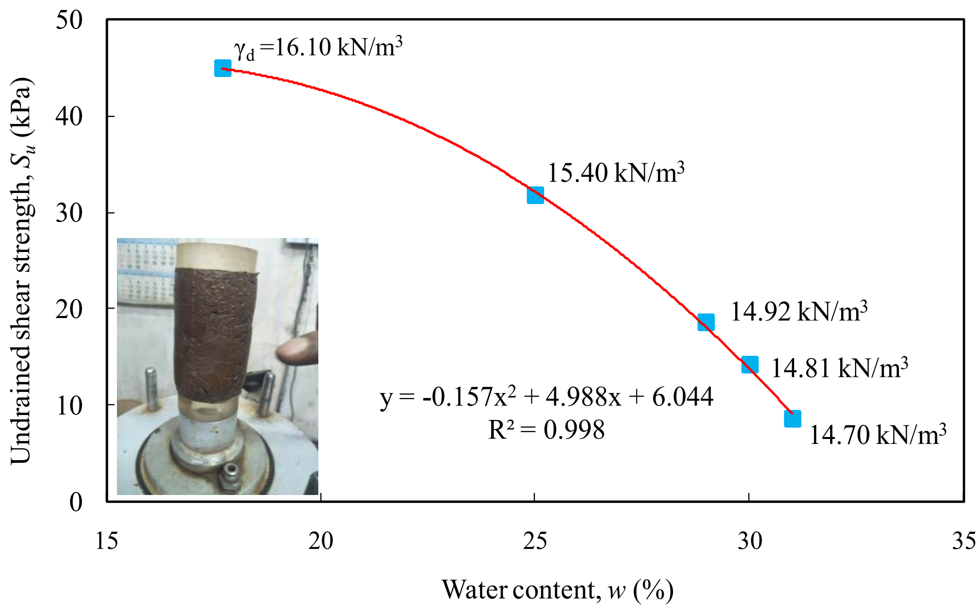

Fig. 3.2(c) Variation of S_u, γ_d of soil with water content, w.

A series of unconfined compressive strength (UCS) tests were carried out on the soil sample, starting at the optimum moisture content (OMC) of 17.7% and progressing up to 31% moisture content. The undrained shear strength of soil (S_u) is 45 kPa at the OMC and 8.5 kPa at 31% water content, which replicates the soft soil condition and remains constant during the entire granular pile experimental process. The soil sample's dry unit weight (γ_d) at corresponding water contents was also calculated. The variation of S_u and γ_d of soil samples with water content (w) is illustrated in Fig. 3.2(c).

The modulus of elasticity of soil (E) is obtained from the deviator stress-axial strain curve of triaxial tests. However, a triaxial test cannot be performed on very soft soils. As an alternative, elastic modulus can be obtained by using an oedometer. The soil sample corresponding to 31% water content (at which S_u= 8.5 kPa) was prepared in an oedometer and compacted to obtain the bulk unit weight of 14.70 kN/m^3, respectively. Since the properties to be determined were undrained, the drainage stone was sealed with polyethylene shrink wrap. The water reservoir was disconnected, and the test was conducted at the existing degree of saturation. A precise dial gauge was attached to note the deformation. A seating pressure of 10 kN/m^2 was applied for 1 min. The pressure was incremented in 10 kN/m^2 intervals, and the corresponding deformation was noted in dial gauges. The deformation noted was instant deformation. The deformation was expressed as a percentage strain corresponding to the initial thickness of the specimen. The slope of the stress-strain curve was determined to obtain the oedometer modulus (E_{oed}).

$$E_{oed}=\frac{(1-\mu)E}{(1-2\mu)(1+\mu)} \tag{3.1}$$

where μ = Poisson's ratio. The Poisson's ratio of very soft soils is in the range of 0.45-0.5, as suggested by (Bowles 1997). The modulus of elasticity of the soft soil is considered 420 kPa by (Hasan and Samadhiya 2016)and 900 kPa by (Ghazavi and Nazari Afshar 2013). Many researchers considered the modulus of elasticity of the soft soils to be less than 1000 kPa. In this study, the soil's modulus of elasticity (E) was 1027 kPa.

Table 3.1 Properties of soil sample used in the study.

Properties	Value
Specific gravity, G_s	2.62
Liquid limit, w_L(%)	33
Plastic limit, w_p(%)	26
Plasticity index, I_p(%)	7
Soil classification	ML
OMC (%)	17.7%
Maximum dry unit weight, $\gamma_{d\,max}$ (kN/m^3)	16.10
$\gamma_d$at 31% water content (kN/m^3)	14.70
$S_u$at 31% water content (kPa)	8.5
Young's modulus of soil, E (kPa)	1027

3.2.2 Aggregates

According to previous studies, the sizes of the aggregates employed in model studies vary between 2 mm and 12.5 mm (Ambily and Gandhi 2007; Murugesan and Rajagopal 2007; Ali et al. 2012). This study used uniform aggregates, angular in shape, with particle sizes ranging from 10 mm to 12.5 mm, for granular pile material, as shown in Fig. 3.3. The aggregates are categorized as GP (poorly graded gravel). The aggregates of the required sizes were collected from Varanasi, Uttar Pradesh, India. The maximum dry unit weight (γ_{dmax}) and minimum dry unit weight (γ_{dmin}) of aggregates are 17.25 kN/m^3 and 14.60 kN/m^3. The aggregates are compacted with a relative density (I_D) of 70%. The corresponding γ_d is 16.36 kN/m^3. The grain size distribution curve of the aggregates is represented in Fig. 3.2(b).

Fig. 3.3 Aggregates used in the present study.

3.2.3 Recycled tire chips

The tire materials of uniform sizes 10 mm × 10 mm × 10 mm were manually shredded/recycled from old worn-out tires and employed as a substitute for aggregates, as shown in Fig. 3.4(a). The tire chips selected should closely match the size of aggregates to ensure performance comparisons. The tire materials utilized in this research are classified as tire chips in accordance with ASTM D6270 (2017). The tire chips were shredded after manually removing steel meshes from old, worn-out tires. Due to manual cutting process, there is a slight variation in the sphericity of tire chips. The size of the tire chips usually varies by ±1.0 mm rather than being precisely 10 mm. However, the effects of shape, size, and orientation of tire chips and aggregates have not been considered for the present study, which could be the scope of future research work. The γ_{dmax} and γ_{dmin} of tire chips are 7.20 kN/m^{3}and 6.00 kN/m^3. The tire chips were compacted with a relative density (I_D) of 70%. The corresponding γ_d is 6.91 kN/m^3. Fig. 3.4(b) illustrates the tire chips - aggregates mixture employed in the present study. The basic properties of tire chips and aggregates are presented in Table 3.2.

Fig. 3.4(a) Tire chips used in the present study.

Fig. 3.4(b) Tire chips – aggregates mixture used in the present study.

Table 3.2 Properties of aggregates and tire chips

Properties	**Aggregates**	**Tire chips**
Specific gravity, G_s	2.73	1.14
$\gamma_{d\,max}$ (kN/m^3)	17.25	7.20
γ_{dmin} (kN/m^3)	14.60	6.00
Relative density, I_D (%)	70	70
γ_d(kN/m^3)	16.36	6.91

3.2.4 Sand

The sand used in this investigation was clean river sand collected from Ganga's banks in Varanasi, Uttar Pradesh, India. The sand particles of size range between 2 mm to 4.75 mm should be used as a sand bed, as shown in Fig. 3.5. The shear strength parameters were determined using direct shear tests. The internal friction and dilation angles were 34° and 4°, respectively. The μ of sand is taken as 0.3 (Bowles 1997). The grain size distribution curve of the sand is represented in Fig. 3.2(b).

Fig. 3.5 Sand used in the present study.

3.2.5 Tire chips - aggregates mixture

Since the index properties (unit weight, specific gravity of tire chips, and aggregates) are entirely different, a regular weight mixing procedure has not been adopted. Volume batching was used to mix aggregates and tire chips, as explained by (Bali Reddy et al. 2016). The mix proportions employed in the current research are presented in Table 3.3. The notations will remain consistent throughout the subsequent chapters.

Table 3.3 The mix proportions of tire chips and aggregates.

S. No.	Mix Proportions (by weight batching)	Notation used
Mixture 1	(0% tire chips + 100% aggregates)	(0% TC + 100% AG)
Mixture 2	(25% tire chips + 75% aggregates)	(25% TC + 75% AG)
Mixture 3	(50% tire chips + 50% aggregates)	(50% TC + 50% AG)
Mixture 4	(75% tire chips + 25% aggregates)	(75% TC + 25% AG)
Mixture 5	(100% tire chips + 0% aggregates)	(100% TC + 0% AG)

3.2.5.1 Specific gravity of tire chips - aggregates mixture

Specific gravity (G_s) values of tire chips-aggregate mixtures were determined as per IS 2386- Part III (1963). Three samples were made from each mix proportion for average G_s value. (Bali Reddy et al. 2016) derived a formula for the calculation of the specific gravity for a mixture (G_m) of sand and tire knowing the specific gravity values of sand and tire chips alone along with individual weights in the mixture as:

$$G_{m\,(cal)} = \frac{W_m}{\left(\frac{W_{tc}}{G_{tc}} + \frac{W_{ag}}{G_{ag}}\right)} \tag{3.2}$$

Fig. 3.6 shows G_s values determined in the laboratory for all mix proportions with tire content and G_m values calculated using Eq. 3.2, which agree with each other. The range of specific gravity values for tire chips was reported to be 1.02 – 1.24 in the literature (Humphrey 1999; Ahmed 1993). The specific gravity value of pure tire chips obtained in the present study is 1.14.

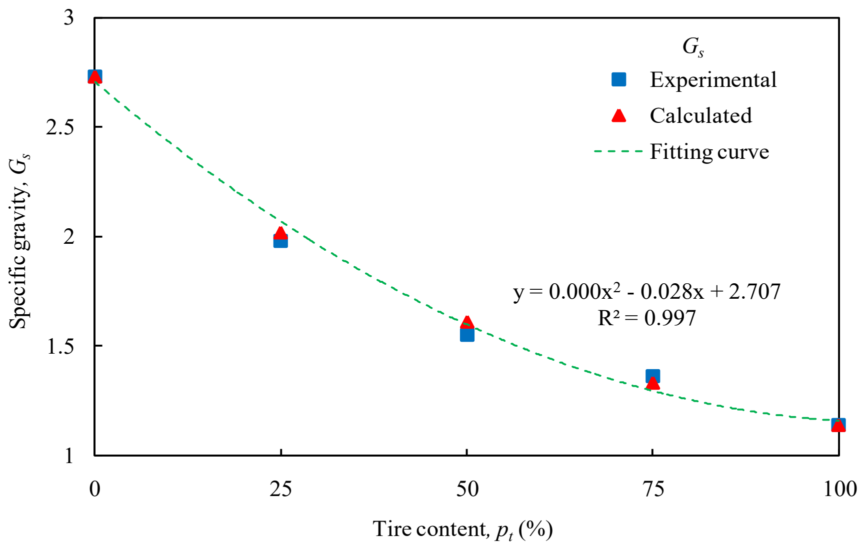

Fig. 3.6 Specific gravity values of tire chips - aggregates mixture.

The calculations for volume batching are as follows:

The following is the mix proportion (25% TC + 75% AG).

(25% TC + 75% AG) on a weight basis,

$$\% W_{tc} = \frac{W_{tc}}{W_{tc} + W_{ag}} \tag{3.3}$$

(25% TC + 75% AG) on a volume basis,

$$\% V_{tc} = \frac{\frac{W_{tc}}{G_{tc}}}{\frac{W_{tc}}{G_{tc}} + \frac{W_{ag}}{G_{ag}}} \tag{3.4}$$

According to the above calculations, the tire chips percentage of 25% by weight is equivalent to 44.4% by volume. Similarly, the tire chips percentage of 50% by weight and 75% by weight is equivalent to 70.5% and 87.8% by volume, respectively. The correlation between volume mixing and weight mixing of tire chips and aggregates is presented in a graphical form, as shown in Fig. 3.7.

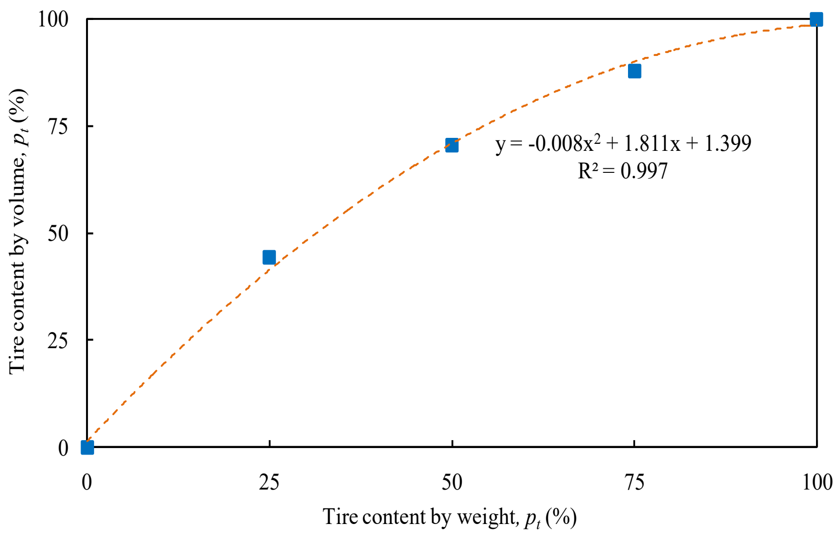

Fig. 3.7 Relationship between volume and weight proportions of tire chips and aggregates mixture.

3.2.5.2 Unit weights of tire chips - aggregates mixture

The maximum and minimum dry unit weights of aggregates and tire chips mixture were determined using IS 2386- Part III (1963). The mix proportions were filled in the tank with an internal diameter of 250 mm and height of 300 mm. The tank size is suitable for aggregates ranging between 4.75 mm to 40 mm. All the mix proportions were oven-dried before the test.

To determine maximum dry unit weight, the mix proportion was filled about the one-third depth of the test tank and tamping with 56 blows using the modified Proctor compaction hammer that weights 4.53 kg and continued until the top of the tank. To determine the minimum dry unit weight, the mix proportion was filled in a test tank from a free height of 5 cm and continued until the top of the tank. The excessive material was struck off using a straight edge. The weight of the material with the tank and the volume of the tank were determined for dry unit weight calculation. (Frikha et al. 2015) have reported that it is difficult to build a coherent granular pile with a relative density greater than 80%; thus, the dry unit weights of all mix proportions were determined at 70% I_D. For aggregate and tire chips mixture beyond 50% tire content, compaction issues occurred due to higher tire chips content by volume than aggregates, which necessitates careful compaction to obtain uniformly compacted samples. The mixing of aggregates and tire chips was already explained in the previous section.

3.2.5.3 Large direct shear test set-up and experimental procedure

Large direct shear tests (305 mm × 305 mm × 200 mm) were conducted to assess the shear behavior of all the five mix proportions employed in this research. Fig. 3.8(a) represents a large direct shear set-up with accessories used for the present work. To prevent boundary effects, the maximum size of granular material should be less than at least one-tenth of the size of the shear box ASTM D3080 (2012). However (Tweedie et al. 1998) contend that the size of granular material that is one-fourth of the size of the shear box contains bigger particles, such as aggregates and tire chips. The above conclusions were supported by (Zahran and El Naggar 2020; El Naggar et al. 2021).They recommended using particles with an aspect ratio less than one-fourth the size of the shear box to eliminate the influence of the shear box's size when evaluating the shear strength parameters of aggregate and tire chip mixtures.

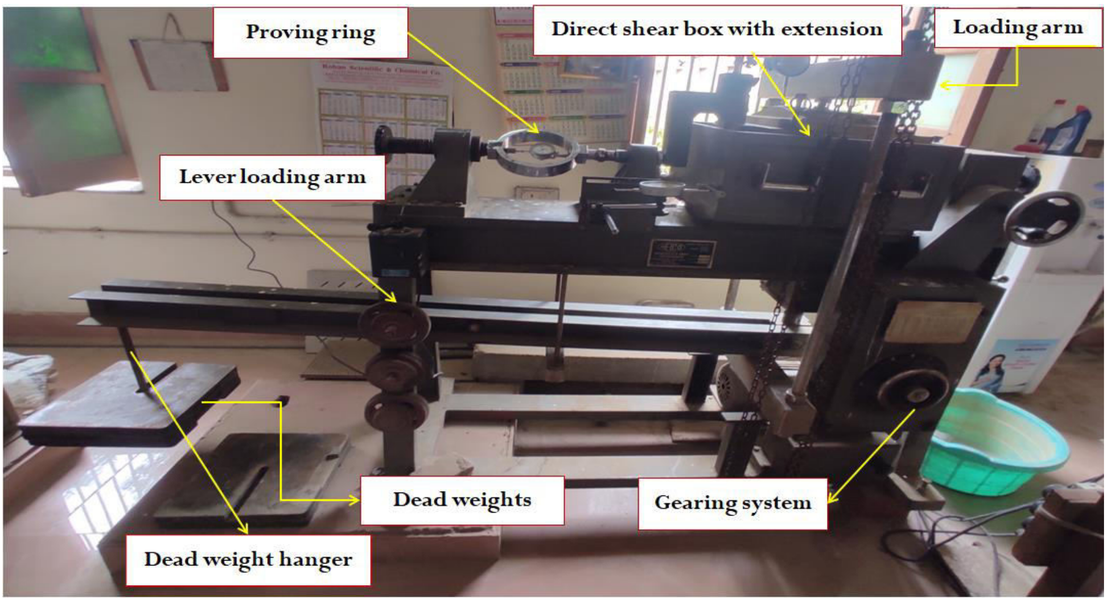

(a)

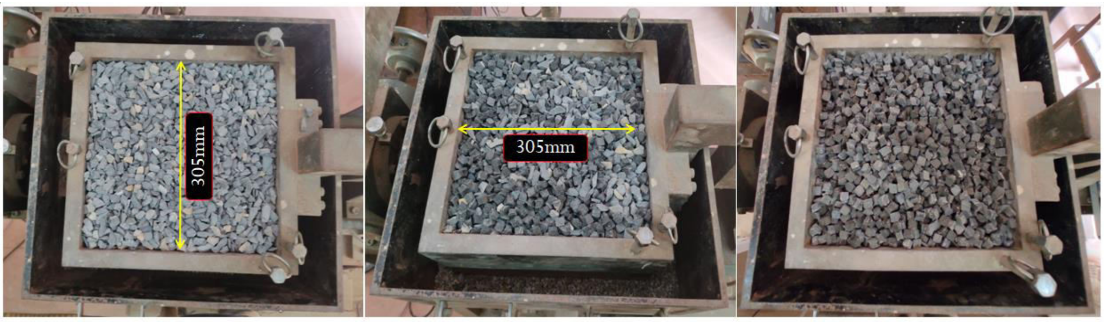

(b) (c) (d)

Fig. 3.8 Large direct shear test; (a) equipment with accessories, (b) shear box with 100% aggregates, (c) shear box with tire chips - aggregates mixtures, and (d) shear box with 100% tire chips.

To prepare the samples, the unit weights of tire chips and aggregates mixture at 70% I_D. The volume of the shear box was used to calculate the amount of mixture in each proportion. The mixture was gradually poured into the shear box in three layers. Each layer was compacted using the same procedure adopted in unit weight tests. The compacted mixture in the large direct shear box is shown in Figs.3.8(b), 3.8(c) and 3.8(d). They represent the shear box with 100% aggregates, tire chips - aggregates mixture, and 100% tire chips.

Direct shear testing was performed in compliance with the accepted test method specified by ASTM D3080 (2012). The device comprises a steel box with a 9 mm thickness and nominal dimensions of 305 mm square, as indicated in Fig. 3.8(a)**.** The shear box's lower half was 90 mm in height, resting on a base support, and the upper half box was 90 mm in height. The shear box was modified, and a loading plate of thickness 30 mm was placed above the upper half of the box to handle the large compressibility of the aggregates and tire chips mixture while being sheared. Dead weights were imparted to apply normal stresses to the specimens, which a lever loading arm then transferred to the top of the specimens. It should be noted that a loading plate was placed before the loading arm was positioned, and the mixture was subsequently subjected to normal stress. The lower half was fixed, while the upper half could move at a controlled speed under the control of an electric motor to shear the material inside. A proving ring with a dial gauge was mounted to quantify the shear force. Two additional dial gauges were fitted to track the vertical and horizontal deformation.

3.2.6 Encasement materials

This study has considered three varieties of geosynthetic materials with different tensile strengths as an encasement for granular piles. The three encasement materials are geotextile (GT), geo-grid (GG), and combi-grid (CG), respectively. The pictorial representation of all three encasements is shown in Fig. 3.9(a). The tensile strengths of the above respective materials are 9.70 kN/m, 14.5 kN/m, and 30 kN/m, respectively. The same notations are used for three encasements in further studies. Many researchers with GT and GG have carried out extensive research work as encasement materials for granular piles. Geogrids are designed to provide significant reinforcement to granular materials, improving load distribution and reducing deformation. This is particularly valuable for enhancing the load-bearing capacity of granular piles. Geotextiles are effective at preventing surrounding soft soil intrusion into the granular piles. They serve as a filter, preventing the mixing of fine soil particles with the granular piles, and geotextile encasement is relatively easy to install, making it a practical choice for various geotechnical applications. This study focused on utilizing a new innovative geosynthetic material, combi-grid, a hybrid geosynthetic material with a combination of geotextile and geogrid. A combi-grid with a tensile strength of 30 kN/m and an aperture dimension of 30 mm × 30 mm was used as the main encasement material. For comparison purposes, two model tests were conducted with geotextile and geogrid as an encasement material.

Combi-grid is a new innovative geosynthetic material, a combination of both geotextile and geogrid. It's made of stretched, monolithic polypropylene flat bars with welded junctions and a mechanically bonded filter geotextile welded within the geogrid structure. It offers several advantages over standalone geotextile and geogrid materials to meet the specific requirements of a wide range of geotechnical and civil engineering projects. The major advantage of a combi-grid is a geo-composite stabilization and reinforcement solution. The higher stiffness of the combi-grid efficiently reduces deformations in the subgrade, extending modern infrastructure's service life. It is utilized to reinforce geogrid in civil engineering, landfill engineering, road construction, railway track engineering, ports, and hydraulic engineering for soil stabilization and bearing capacity improvement. It's very fast and easy to install. Despite its numerous merits, few researchers have employed it as an encasement material in laboratory model tests. The ultimate tensile strengths of the above encasement materials were determined as per (ASTM D4595-09 2009), presented in Fig. 3.9(b) and 3.9(c).K.K. Suppliers, Kolkata, India, supplied the encasement materials utilized in this study. The basic properties of all three encasements are presented in Table 3.4.

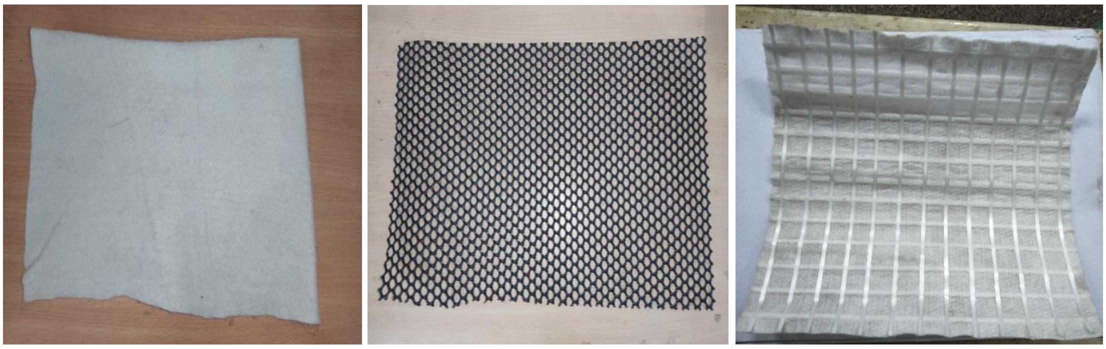

(i) (ii) (iii)

Fig. 3.9(a) Encasement materials used in the study; (i) GT, (ii) GG, and (iii) CG.

Fig. 3.9(b) Wide width tensile strength test.

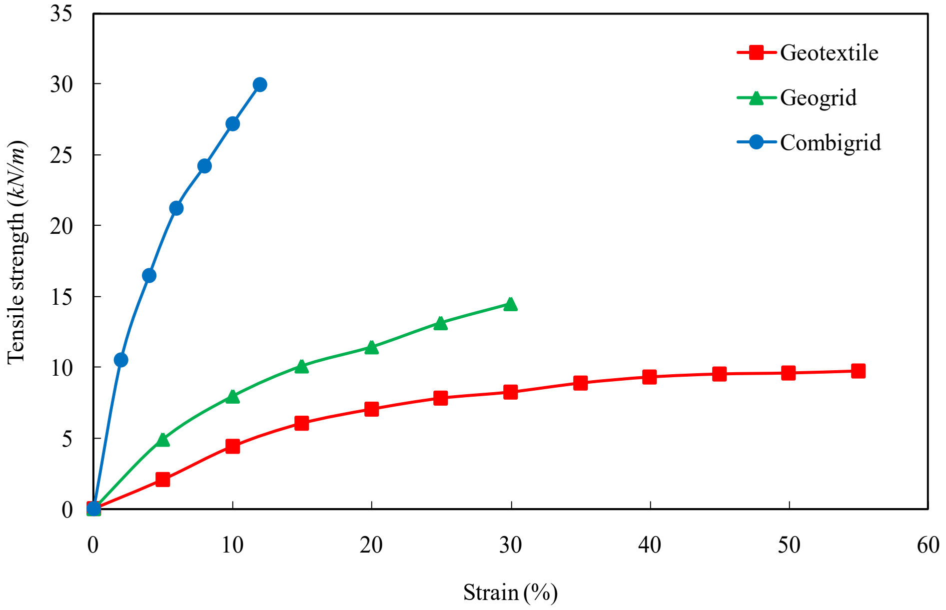

Fig. 3.9(c) Tensile strength-strain behavior of encasement materials.

Table 3.4 Properties of encasement materials.

Properties	Material 1	Material 2	Material 3
Material type	geotextile (GT)	geogrid (GG)	combi-grid (CG)
Ultimate tensile strength (kN/m)	9.7	14.5	30
Strain at ultimate tensile strength (%)	55	30	12
Physical picture			

3.3 Model test procedures for single granular pile

All the laboratory model tests were conducted in the Department of Civil Engineering, IIT BHU, India. Analyzing the behavior of real-life constructions poses challenges due to the significant time and financial investments required. While providing valuable data, full-scale field tests are costly, and only a limited number of such tests have been reported in the literature. Considering these limitations, reduced-scale physical model tests are often selected. Model testing findings are vital to assessing the performance of the prototype ground and establishing analytical and numerical findings. This section describes the model test set-up, modelling considerations, preparation of models and the test procedure, soft bed preparation, static and cyclic loading test variables, model test series, and installation of various sensors/transducers.

3.3.1 Preparation of model test tank

A square steel model test tank with inner sides of 300 mm, depth of 500 mm, and thickness of 5 mm sealed at the bottom and open at the top was used in this research for single granular pile tests, as illustrated in Fig. 3.10(a). Metallic handles were installed for ease of use in that tank. The dimensions of the model tank were carefully chosen to ensure that the failure wedge of the tested granular pile would not interact with the tank's sidewalls. To achieve this, (Meyerhof and Sastry 1978) recommended that the failure zone extend over a radial distance of about 1.5D from the periphery of the granular pile (= 90mm). Moreover,(Ali et al. 2012) established that the in situ stresses should become insubstantial (i.e., less than 10%) at the tank boundaries by assuming an equivalent footing at the two-thirds depth of the granular pile and 2V:1H spread.

Two different recommended minimum sizes for the test tank were referenced in the literature: (Meyerhof and Sastry 1978) suggested a minimum size of 240 mm × 240 mm, while (Ali et al. 2012) recommended a slightly smaller tank size of 200 mm × 200 mm. In this study, the selected size of the model tank was 300 mm × 300 mm. Notably, this selection satisfied both conditions outlined in the previous recommendations, as illustrated in Fig. 3.10(b).

(a)

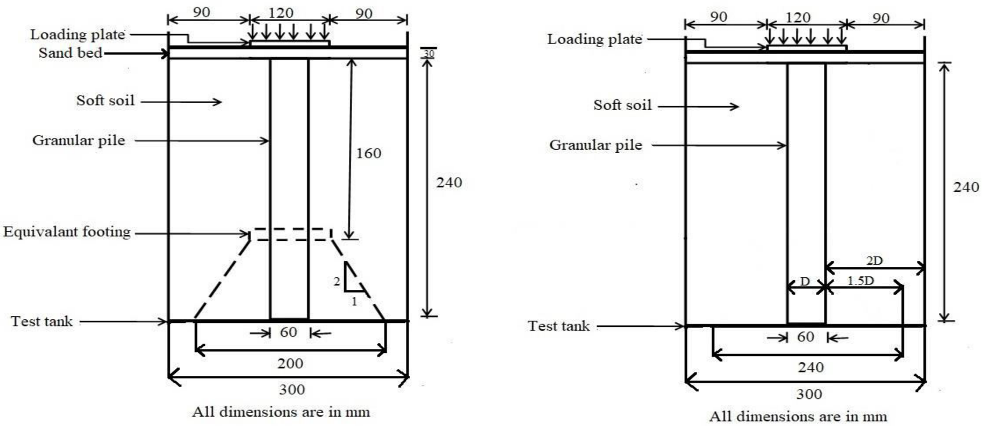

(b)

Fig. 3.10 (a)Model test tank, and (b) Criteria for selection of test tank.

3.3.2 Preparation of soil bed

Soft soils usually have a S_u value of less than 10 kPa (Ali et al. 2014). In all experimental investigations, the soil bed's undrained shear strength (S_u) was prepared at 8.5 kPa, resembling very soft field conditions. Multiple trial and error unconfined compression test iterations were undertaken to ascertain the amount of water needed to be mixed with the dry soil to create a soft soil bed with the desired shear strength of 8.5 kPa. The required shear strength was achieved with a water content of 31%. Before the slurry preparation, the soil underwent drying in an oven for 48 hours at

105°C to prevent biological processes (Ullah et al. 2022). Dry silty soil was meticulously blended for a minimum of 15 minutes at this specific water content using a mechanical soil mixer to produce a homogeneous paste, as shown in Fig. 3.11.

Fig. 3.11 Mechanical soil mixing machine for preparing soil paste.

Before transferring the soil paste into the model test tank, a smooth polyethylene sheet was applied to the inner surface of the tank walls, followed by a thin layer of silicone grease to minimize friction against the walls. Afterward, the test tank was filled with the soil paste in 8 layers, each measuring 30 mm in thickness, and sensors for pore pressure and earth pressure were installed at the appropriate depths. After the soft bed was prepared up to the required level, it was kept uninterrupted for 48 hours to restore thixotropic strength. A damp jute cloth was used to cover the tank to avoid moisture loss.

3.3.3 Installation of the ordinary granular pile (OGP)

Granular piles were installed in the laboratory model studies by different methods like replacement, displacement, compaction, and frozen columns (Sivakumar et al.

2004; Madun et al. 2012; Wood et al. 2015; Yoo and Abbas 2020). In this research, the replacement technique was followed, considering this method is the most efficient (Ghazavi and Nazari Afshar 2013; Hasan and Samadhiya 2018; Nazariafshar et al. 2019; Yoo and Abbas 2019; Zhang et al. 2020; Gao et al. 2021). Defining scaling laws between prototype and model dimensions is important in laboratory model testing. In this study, the scale factor is typically decided based on the granular pile length to granular pile diameter (*L/D* ratio) of prototype and model studies as per the procedure of scaling explained by (Gniel and Bouazza 2009). Using a single scaling factor to model the range of different diameters of granular piles may be difficult. However, the model scale (1/λ) is considered 1/10 in this study. In the field, the diameters of proto-type granular piles vary from 550 mm to 1200 mm. The model studies' diameter ranges from 55 mm to 120 mm. The diameter of the granular pile (*D*) considered in this study is 60 mm.

The *L/D* ratio of granular piles considered is in the range of 4 to 10 from prior research (Greenwood 1970; Hugher and Withers 1974; Murugesan and Rajagopal 2006; Malarvizhi and Ilamparuthi 2007; Black et al. 2011; Dash and Bora 2013; Basu et al. 2018). (Hugher and Withers 1974) was the first person to establish the *L/D* ratio and observed that there is no increase in the ultimate bearing capacity of the granular pile with an *L/D* ratio higher than 4.1. (Basu et al. 2018) examined the influence of the *L/D* ratio on the ultimate bearing capacity of the granular pile and observed that the critical length of the granular pile is 3D, beyond which there is a negligible increment in the ultimate bearing capacity. (Black et al. 2011) concluded that settlement can be controlled in short granular piles with *L/D* < 6 at high area replacement ratios. Considering the above conclusions, the granular piles with *L/D* ratios of 4, 5, 6, and end-bearing conditions were considered in this study.

A wooden frame of 300 mm × 300 mm × 10 mm with a prefabricated hole of 60 mm diameter at the center was used to install a granular pile, as shown in Fig. 3.15.A slender open-ended perspex tube with an internal diameter equal to the desired diameter of 60 mm was then gradually pushed into the soft bed through a pre-fabricated hole until it reached the base plate, ensuring an end-bearing condition. A thin silicon grease coat was spread over the inner and outer surfaces of the perspex tube before insertion to reduce friction between the tube and the soil. The soil within the perspex tube was extracted using a specially made auger, while the tube was retained in situ. It was very tough to install a granular pile with a relative density (I_D) above 80% (Frikha et al. 2015). The mixture's relative density (I_D) in a granular pile is made at about 70% (Gao et al. 2021). Attaining a compaction relative density (I_D) of 70% with elastic materials such as tire chips is indeed challenging. The required compaction can be achieved by layering the tire chips and aggregates mixture in increments and compacting each layer separately. The calculated quantities of all five mix proportions of tire chips- aggregates for granular pile at 70% I_D is depicted in Fig. 3.12.

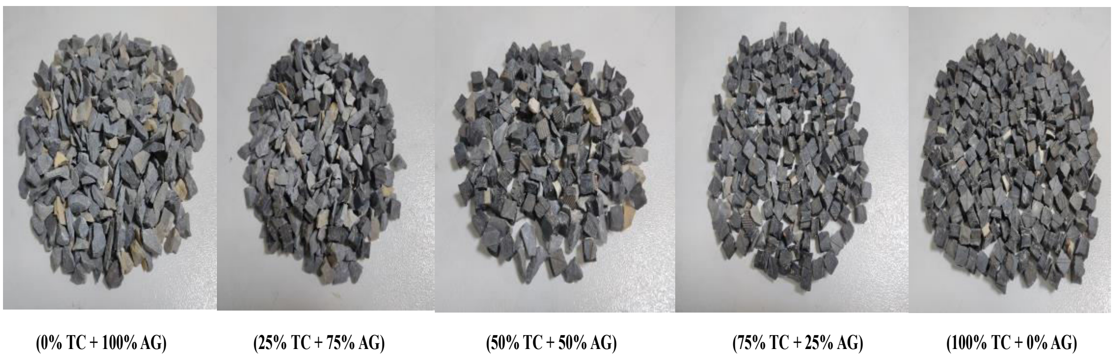

(0% TC + 100% AG) (25% TC + 75% AG) (50% TC + 50% AG) (75% TC + 25% AG) (100% TC + 0% AG)

Fig. 3.12 Pictorial representation of five mix proportions of tire chips and aggregates for granular piles.

The tire chips - aggregates mixture was placed into a perspex tube in 30 mm layers and compacted with a tamping rod for each layer. After compacting each layer, the tube was slowly raised, maintaining a minimum overlap of 10 mm. Repeat the same procedure till it reaches 240 mm. Multiple compaction cycles are necessary to achieve the desired relative density, especially when dealing with elastic materials.

3.3.4 Installation of geosynthetic encased granular pile

A similar process of installing ordinary granular piles is followed to install the encased piles. First, the encasement materials (GT, GG, and CG) were wrapped around the perspex tubes of 60 mm diameter and inserted through the prefabricated holes made on a wooden frame. The geogrid encasement was wrapped around the granular pile using the overlapping technique suggested by (Gniel and Bouazza 2010). The technique was to wrap the encasement material around the perspex tube with a required overlap length of 15 mm and sew the overlapping joints with nylon straps. A similar technique was implemented by (Mazumder et al. 2018; Yoo and Abbas 2019; Zhang et al. 2020). The GT was wrapped around the perspex tube with a nominal overlap length of 15 mm, and the overlapping joints were glued and stapled together to create an encasement sleeve. A similar technique was implemented by(Ghazavi and Nazari Afshar 2013; Hasan and Samadhiya 2017; Yoo and Abbas 2020). CG is a combination of GT and GG, so a similar wrapping method of GT was followed, as illustrated in Fig. 3.13.

A similar procedure of VEGP was followed for horizontal encased granular piles (HEGP) and combined encased granular piles (CEGP). In the case of HEGP and CEGP, the encasement is provided as horizontal discs at a spacing of 0.25D, 0.5D, and D (=15 mm, 30 mm, and 60 mm). The determined amount of mixture was placed into a perspex pipe in 0.25D, 0.5D, and D layers and compacted with a tamping rod for each layer. After attaining respective heights, encasement is provided in horizontal discs and repeats the same procedure until it reaches 240 mm. The arrangement of encasement in granular piles is illustrated in Fig. 3.14(a) and Fig. 3.14(b). The sequence of model ground preparation, soft soil bed preparation, and granular pile installation is presented in Fig. 3.15.

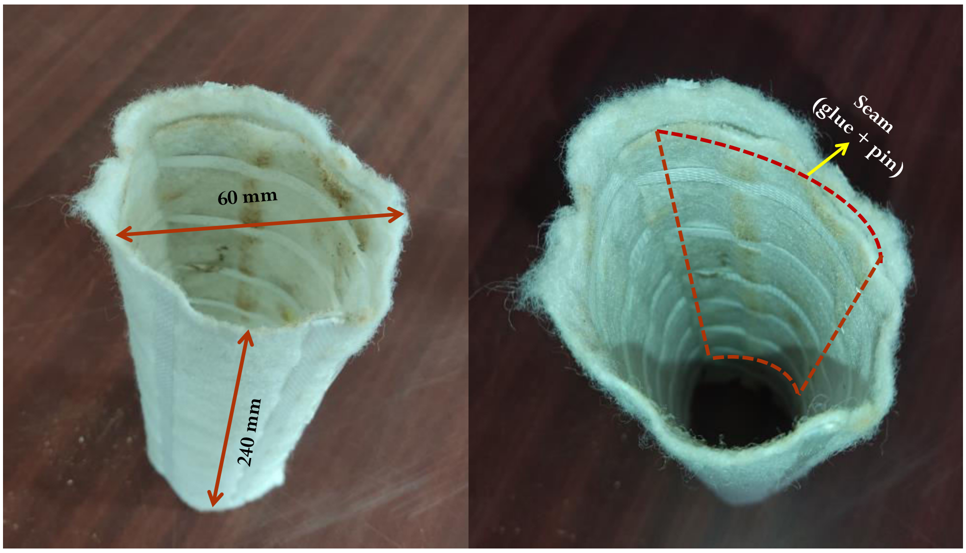

Fig. 3.13 Combi-grid encasement sleeve.

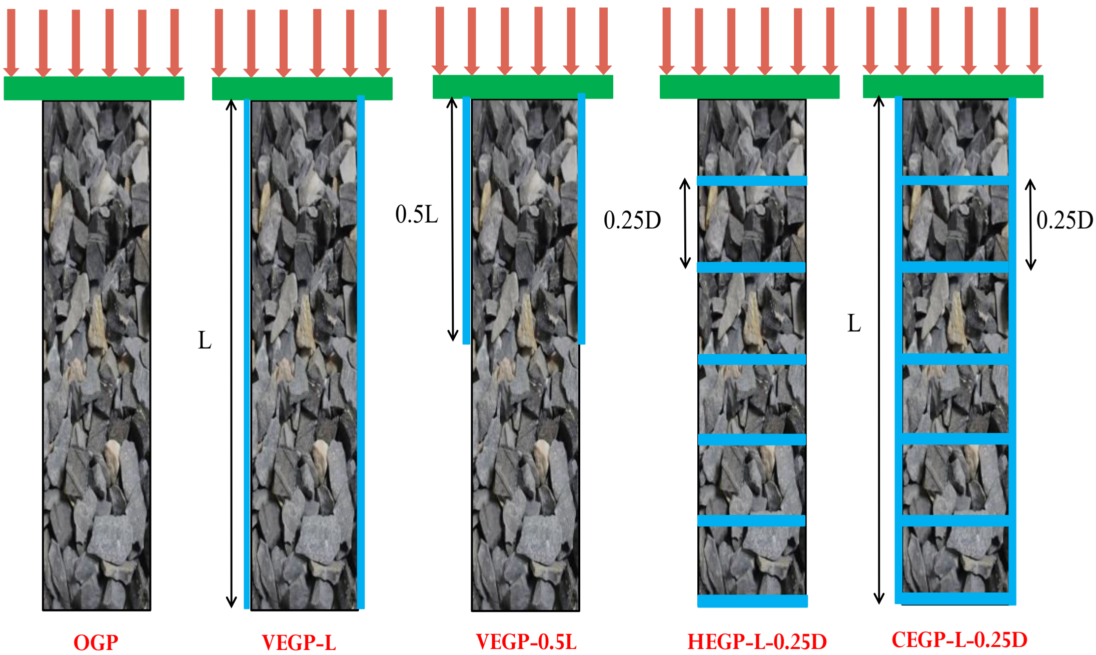

Fig. 3.14(a) Schematic diagram of granular pile under different encasement configurations.

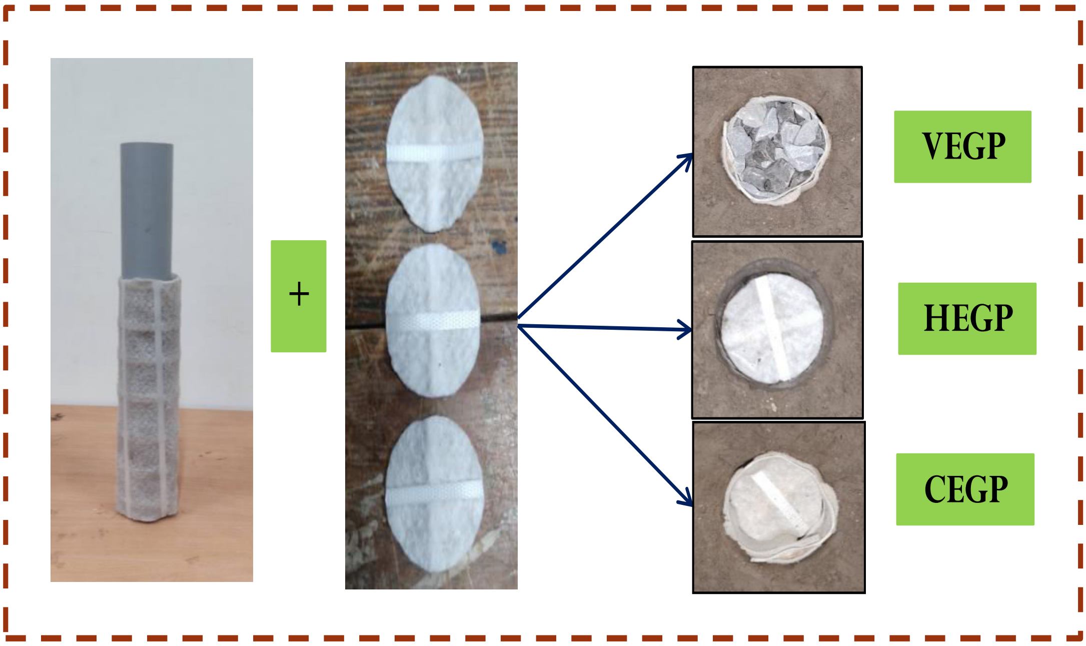

Fig. 3.14(b) Pictorial representation of granular pile under different encasement configurations.

Fig. 3.15 Pictorial representation of model ground preparations including soft bed, granular pile installation along with pore pressure and earth pressure transducers.

3.3.5 Test variables

Laboratory model tests were conducted to analyze granular piles' static and cyclic behavior. Various theoretical models have been proposed to estimate the cyclic stresses at the subgrade level, considering cyclic loading factors such as cyclic loading frequency (f_{cy}) and amplitude (q_{cy}). The cyclic loading characteristics considered in this study were by simulating a sinusoidal loading wave representing the traffic or train loading in terms of train speed, length of train coach, and train axle load, as reported by (Yoo and Abbas 2020; Ashour et al. 2022). The empirical equations to calculate cyclic loading amplitude and frequency are as follows.

$$\sigma_d = 0.26P + 0.26P\alpha V \tag{3.5}$$

$$f = \frac{V}{3.6L} \tag{3.6}$$

where σ_d is the vertical cyclic stress on the subgrade (kPa), P is the train axle load (kN), V is the train speed (km/hr), α is the speed coefficient, and L is the length of the train coach. The average speed, length of the coach, and speed coefficient considered in this study are 90 km/hr, 25m, and 0.003, respectively. In 2009, a decision was made by the Ministry of Railways, Government of India, to improve the soil subgrades for future requirements on Indian Railways, with a design axle load of 25 tons as per (RDSO-GE-0011).So, this study considered the design axial load to be 250 kN. Considering the above values, the q_{cy} and f_{cy} values determined are approximately 85 kPa and 1 Hz, respectively.

A normalized parameter cyclic stress ratio (CSR) is reported by (Zhang et al. 2020), illustrating the cyclic loading amplitude on a granular pile and is defined as

$$CSR = \frac{q_{cy}}{q_{us}} \tag{3.7}$$

where q_{cy} is the cyclic load amplitude, and q_{us} is the ultimate bearing capacity of an OGP in static conditions. The ultimate bearing capacity of an OGP with (0% TC +

100% AG) is taken as a reference at 50 mm settlement. This study takes a cyclic load amplitude of 85 kPa, corresponding to a CSR value of 0.65. Considering CSR value in the broad spectrum of 0.5 to 0.8 could facilitate classifying the threshold amplitude level for granular pile-reinforced soils (Ashour 2015).

The number of cycles or load applications considered in cyclic loading ranges between 500 to 10,00,000 based on material and equipment limitations (Ashour 2015). In this study, the number of loading cycles (*N*) considered was 5000 in all experiments, considering the limitations of test equipment.

3.3.6 Loading and Instrumentation

Prior to loading, a 30 mm thick sand mat with a relative density of 70% was placed over the granular pile installed soil bed. For single granular pile models, the diameter of the loading plate was determined according to the diameter of the granular pile and the area replacement ratio (A_r). The area replacement ratio is defined as the ratio of the granular pile area to its tributary area. In the case of single granular piles, the tributary area is assumed to equal the diameter of the loading plate (D_p). (Barksdale and Bachus 1983) reported that granular pile material typically substitutes 15% to 35% of the soil volume in granular pile-improved foundations. A circular steel plate of 120 mm diameter was employed as a model loading plate for an A_r of 25% corresponding to a granular pile diameter of 60 mm and placed above the sand bed for loading. The center of the loading plate and load cell would coincide. Also, the loading plate was sufficiently rigid, ensuring that no differential settlement was observed during the tests. The strain-controlled mode was used for static loading tests, whereas the stress-controlled mode was used for cyclic loading tests. In strain-controlled tests, the loading is applied at a strain rate of 1 mm/min to ensure undrained conditions (Ali et al. 2014), and the loading plate was subjected to a maximum settlement of 50 mm (Murugesan and Rajagopal 2007; Ghazavi and Nazari Afshar 2013).

This study used a multi-purpose, 20 kN capacity, servo-controlled pneumatic loading data actuator to apply static and cyclic compression loading on the model composite foundation. This model set-up included a load cell of 10 KN capacity for measuring stresses and LVDT to measure the loading plate settlement. A three-port digital data logger was employed to record and analyze the cyclic data, which could be visualized on a computer via data collection software. The model test set-up with load cell and LVDT is represented in Fig. 3.16. A comprehensive summary of the cyclic data retrieved from the stress-controlled data acquisition system for the test tank has been plotted in Figs. 3.17(i-iv) illustrates the sinusoidal loading application, variation of q_{cy} with S_c, S_c with N, and q_{cy} with N up to 500 cycles.

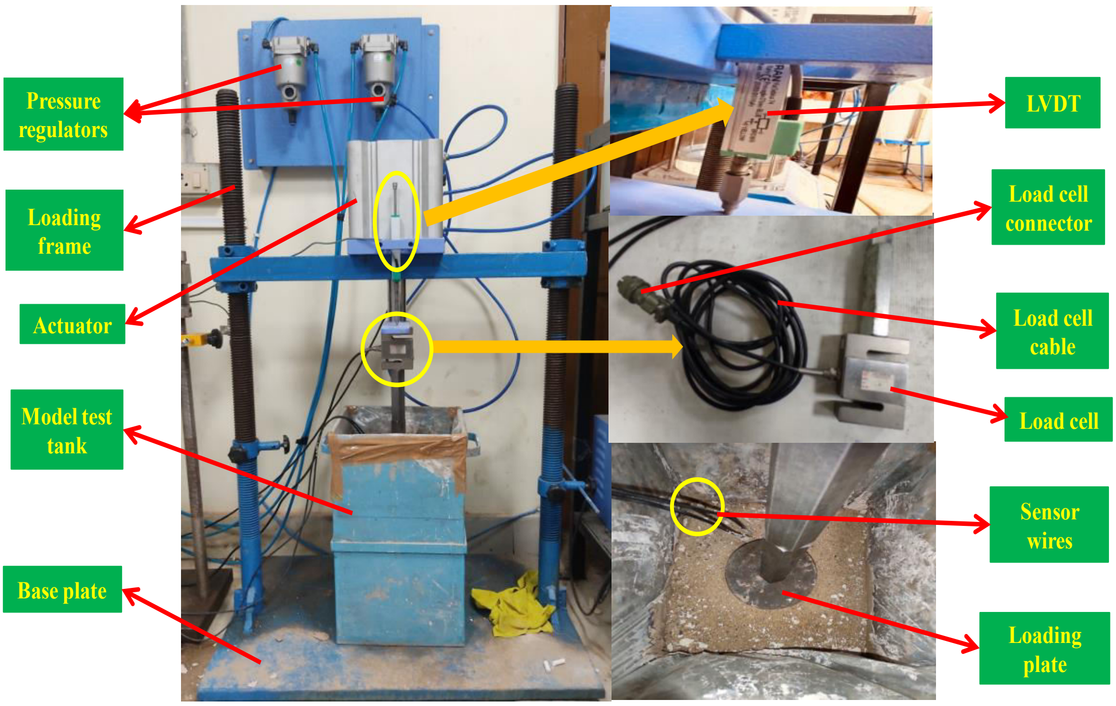

Fig. 3.16 Model test set-up with load cell, and LVDT.

Miniature pore water pressure transducers (PPTs) were embedded in the composite ground to analyze the cumulative excess pore water pressure (P_{exc}) response in the surrounding soil under cyclic loading. The small-sized embedded type PPT (make BPR-A-S, FSO-50 kPa) from PANATACHASIA with a maximum pore pressure capacity of 50 kPa was used to record the pore pressure data. Three PPTs were installed in the test tank at depths of 30 mm, 150 mm, and 270 mm from the loading plate level and 60 mm from the center of the granular pile in lateral direction. P_{exc} data obtained from PPT installed in the middle of the test tank (i.e., 150 mm from the loading plate) are plotted in results and discussions.

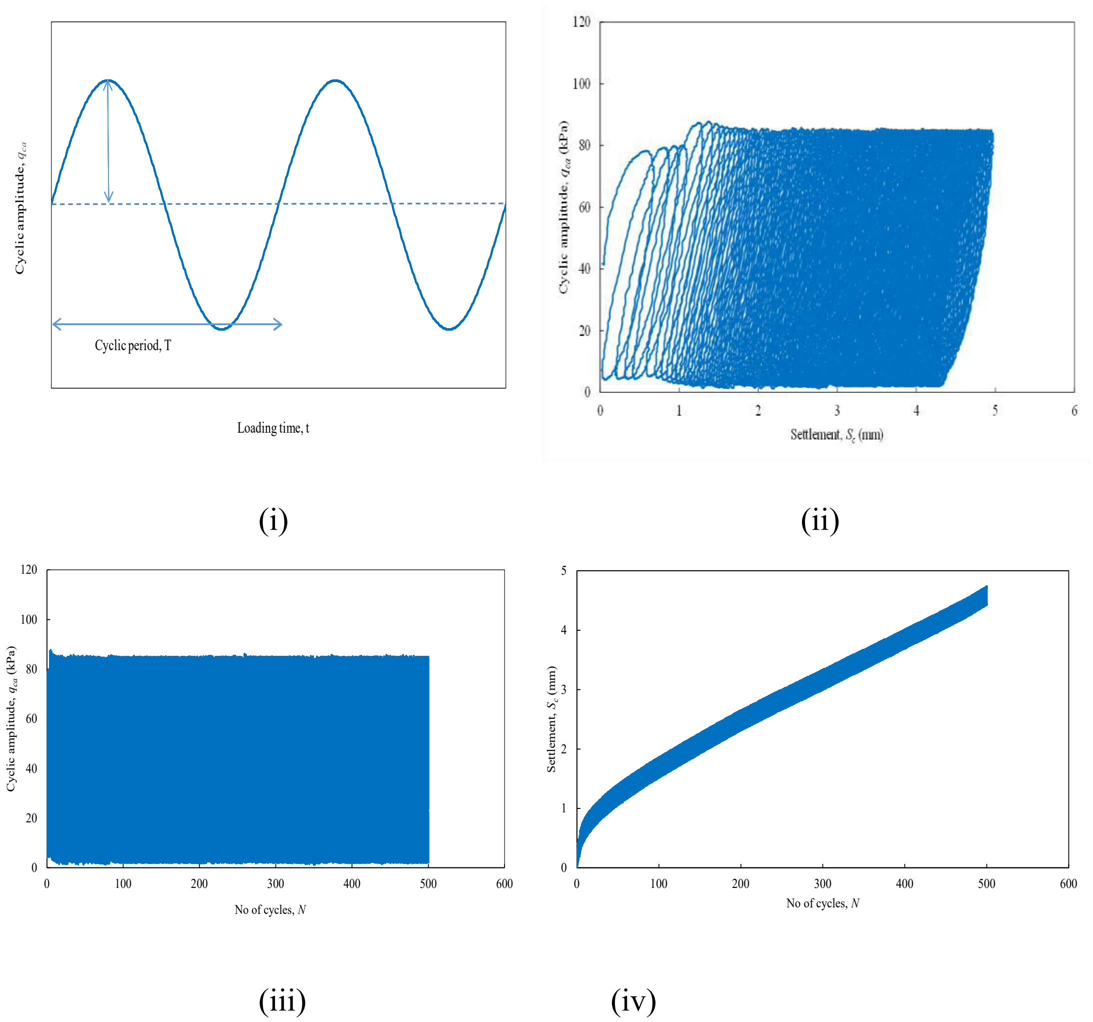

Fig. 3.17 (i) Schematic diagram of sinusoidal loading, (ii) variation of q_{cy} with S_c, (iii) variation of q_{cy} with N, (iv) variation of S_c with N up to 500 number of cycles.

The PPT weighed 50 grams, with a sensing surface diameter of 10 mm and a length of 20 mm. The pore water pressure is measured by a flexible silicon diaphragm present in front of the PPT. The diaphragm is protected from the surrounding soil by a ceramic filter at its front that allows only pore fluid to get through it. Similarly, two miniature earth pressure transducers (EPTs) (make KDE-200 kPa, KDE-1 MPa) from Tokyo Measuring Instruments Laboratories were installed on the granular pile and surrounding soil bed at a depth of 30 mm from the loading plate to record stresses (both σ_{GP} and σ_{SB}) during cyclic loading. The EPTs weighed 160 grams, with a sensing surface diameter of 35 mm and a thickness of 11.3 mm. The arrangement of pore pressure transducers in the model test tank is presented in Fig. 3.18.

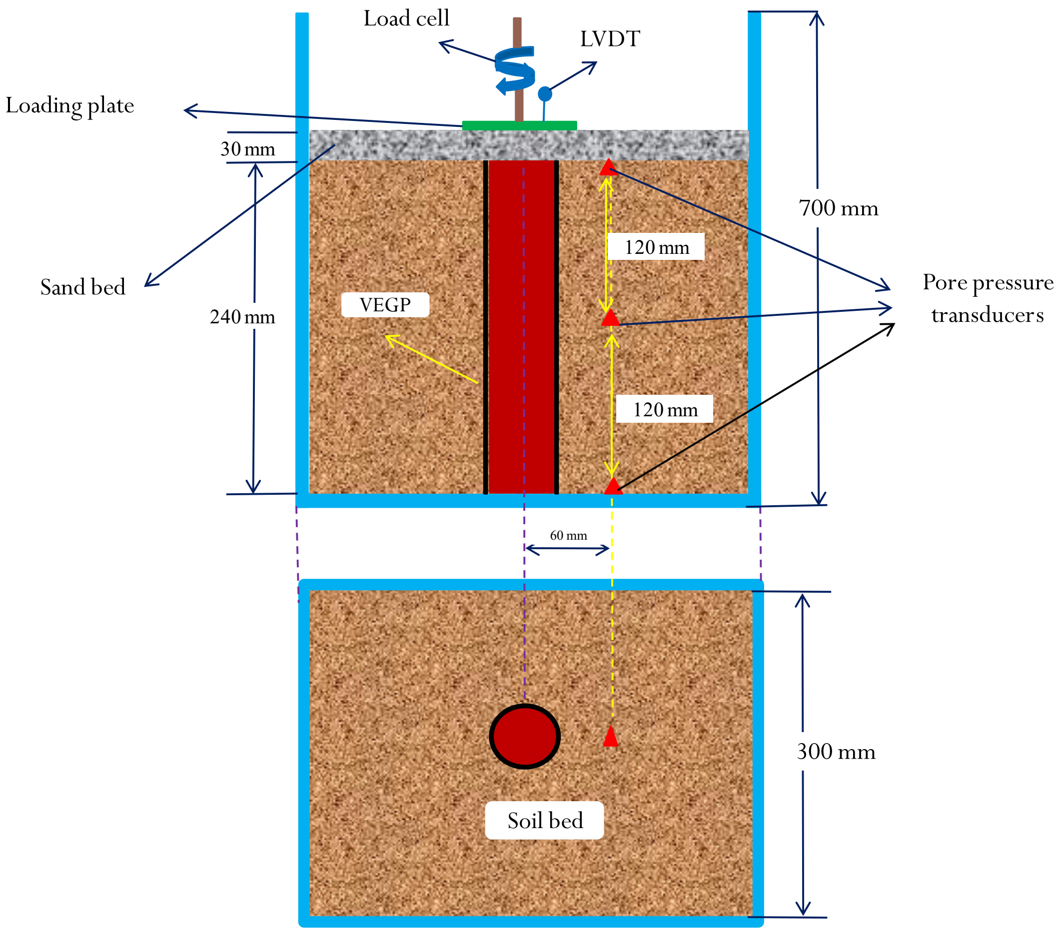

Fig. 3.18 A schematic sketch of the test set-up with PPTs and EPTs.

The data from PPT and EPTs was frequently stored and extracted using a DEWESOFT universal data acquisition system. The visual representation of PPT, EPTs, computers, and DEWESOFT data logger is illustrated in Fig. 3.19.Prior to every model test, all instruments, including load cell, LVDT, and sensors, were properly calibrated.

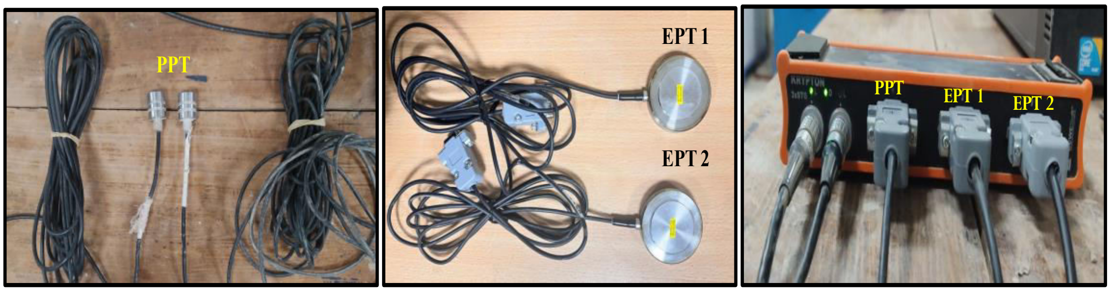

(a) Pore pressure transducers, (b) Earth pressure transducers, (c) Dewesoft data logger,

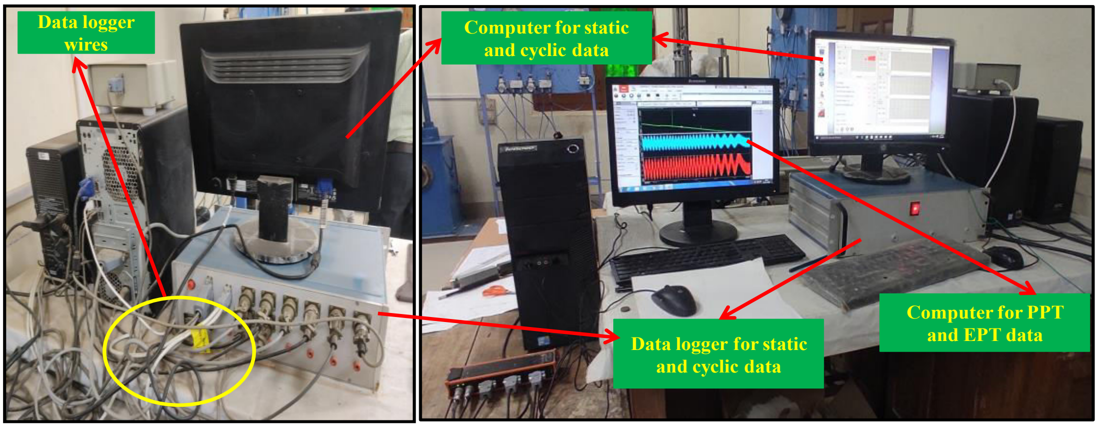

(d) Computer and data loggers for static and cyclic stress data.

Fig. 3.19 Data logger, computer, pore pressure transducers, and earth pressure transducers used in the model study.

3.4 Model test procedures for a group of granular piles under the axisymmetric condition

3.4.1 Preparation of model test tank

A fabricated model test set-up was used in the present study. This set-up comprises a large model test tank and a rigid loading frame with a base plate that supports an actuator. A square steel model test tank with inner sides of 500 mm, depth of 700 mm, and thickness of 5 mm sealed at the bottom and open at the top was used in this research for a group of granular pile tests, as illustrated in Fig. 3.20(a).

Fig. 3.20(a) A schematic sketch of the model test tank.

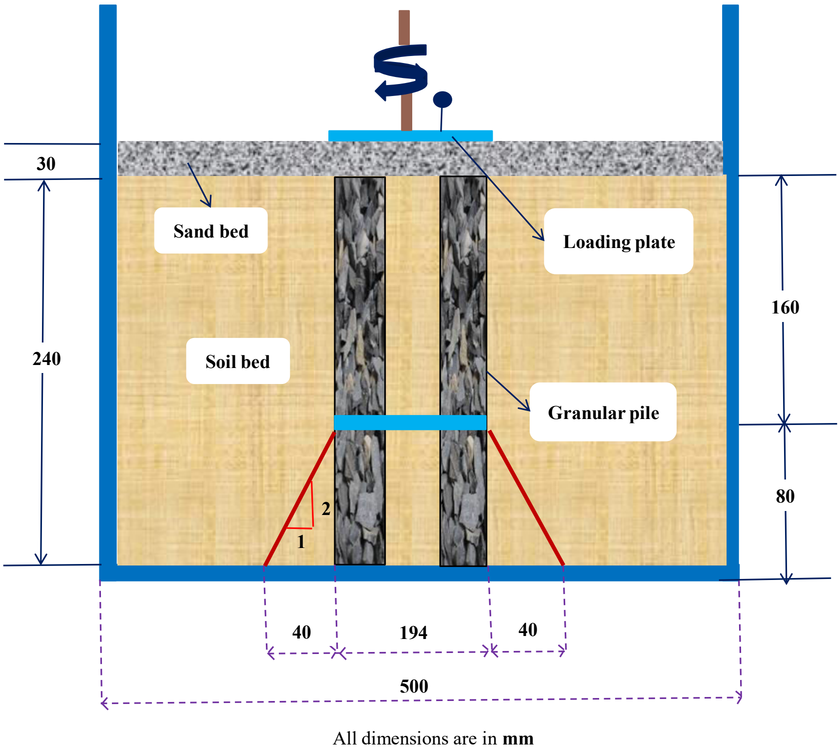

Fig. 3.20(b) A schematic sketch of the model test tank.

The size of the model tank was selected to meet the boundary constraints explained by (Ali et al. 2012), similar to a single granular pile, as outlined in Fig. 3.20(b). The size of the model tank should be carefully selected to prevent the interaction between the failure wedge of granular piles and the test tank side walls. For this, (Ali et al. 2012) proposed that the in situ stresses should become less than 10% at the tank boundaries by assuming an equivalent loading plate located at the two-thirds depth of the granular pile with a spread ratio of 2V:1H. However, the size of the model test tank meets the aforementioned criteria.

3.4.2 Installation of ordinary and encased granular piles

The procedure for preparing the soft soil bed for a group of granular piles is the same as for a single granular pile. A wooden frame of dimensions 500 mm × 500 mm × 10 mm with prefabricated 12 holes was used to install granular piles. The prefabricated 12 holes were made in a triangular pattern similar to (Murugesan and Rajagopal 2010; Ghazavi and Nazari Afshar 2013) for an area replacement ratio of 25%. The wooden frame was placed on top of the soft soil bed. Hollow perspex tubes with an external diameter of 60 mm and inside surfaces coated with silicon grease were inserted through the holes until the base of the test tank reached end-bearing conditions. The soil within the perspex tubes is extracted employing a custom soil extruder built explicitly for this function. The relative density at which the aggregates and tire chips mixture is compacted in a granular pile is 70%.

The quantity of aggregate-tire chip mixture required for each granular pile is calculated as per 70% I_D, as shown in Fig. 3.21. The predetermined quantity of mixture was transferred into a perspex tube in layers of 30 mm each and compacted using a tamping rod for every layer, the same as a single granular pile. The quantity of energy exerted throughout the compaction of the mixture is of major significance. After compacting each layer, the perspex pipe was gradually lifted, ensuring a minimum overlap of 10 mm. Repeat the same procedure for the remaining 11 granular piles. The installation of granular piles follows the pattern from center to outer. A similar process of provision of encasements to a single granular pile is followed for a group of granular piles.

Fig. 3.21 Pictorial representation of tire chips - aggregates mixture for a group of 12 granular piles.

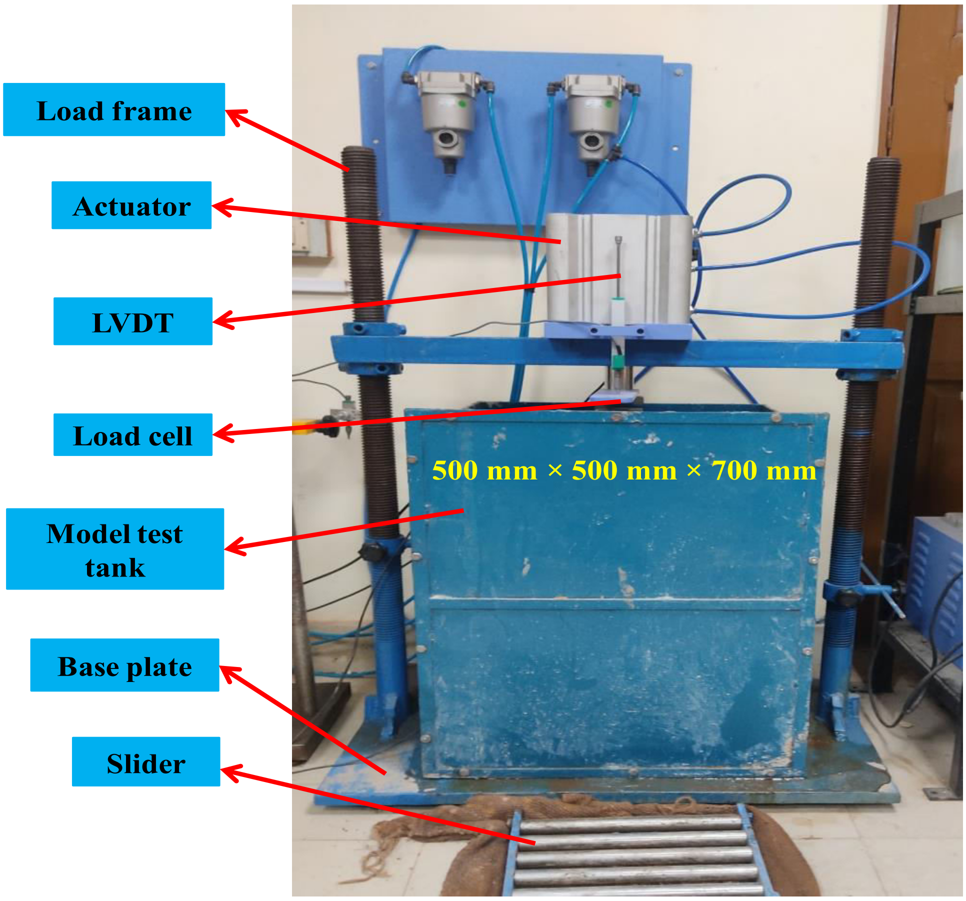

Fig. 3.22 Model test set-up for a group of granular piles.

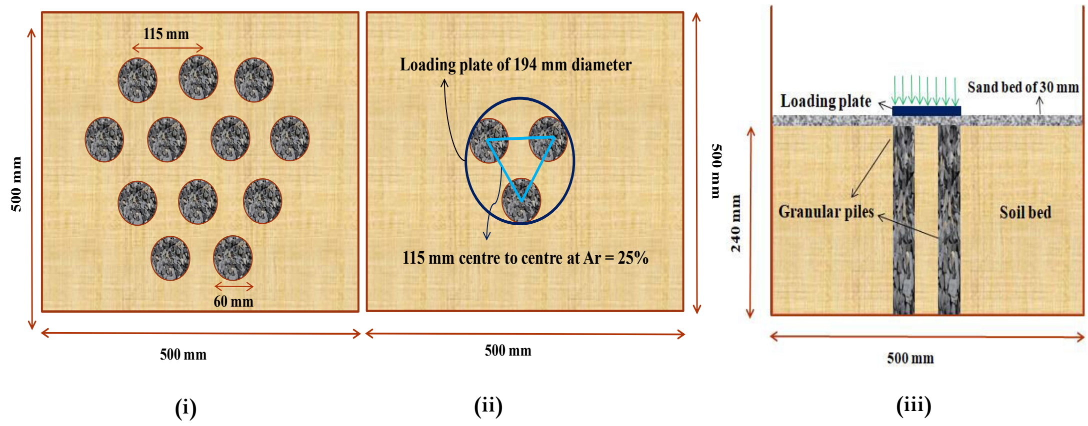

Fig. 3.23 The schematic diagram represents (i) Plan view of the group of 12 granular piles arrangement, (ii) Plan view of the group of three central granular piles with a loading plate, and (iii) Cross-sectional view of the group of central three granular piles with loading plate.

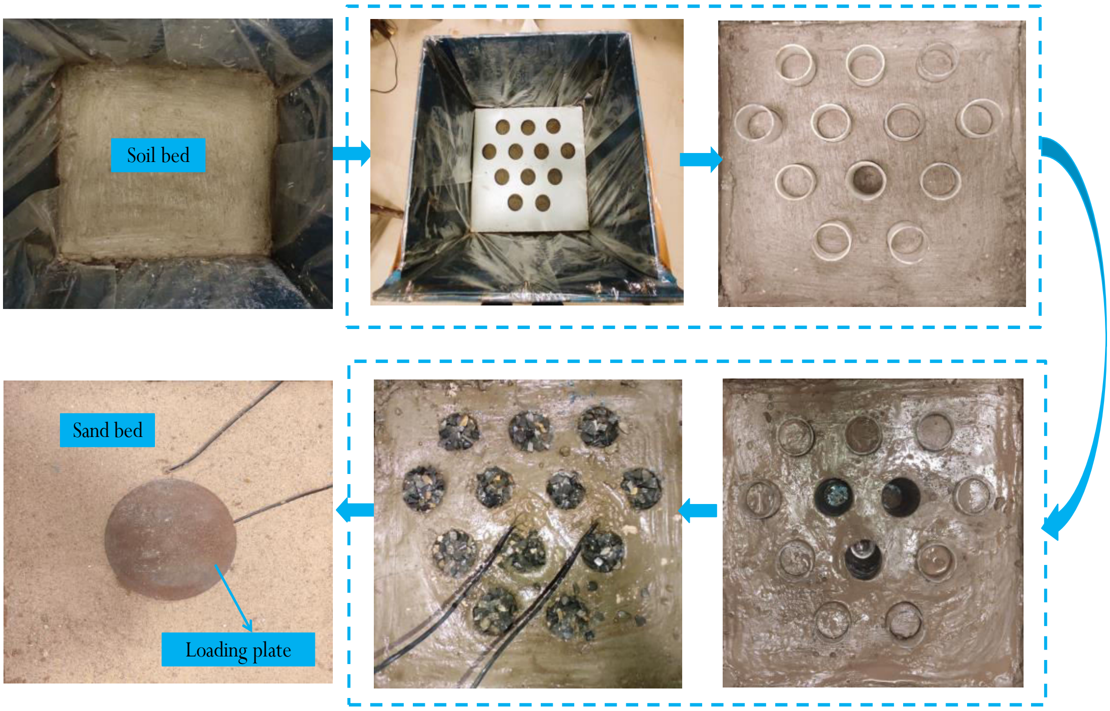

Fig. 3.24 Group of granular piles installation in the model test tank.

Fig. 3.22 represents the model test set-up used for the group of granular piles. Fig. 3.23 presents the schematic sketch of the plan and cross-sectional views of all 12 granular piles and three central granular piles below the loading plate. Fig. 3.24

illustrates the schematic and pictorial representation of model test procedures, including soil bed preparation and installing a group of granular piles.

3.4.3 Instrumentation and loading procedure

For static and cyclic loading on the granular piles, a multi-functional, servo-controlled pneumatic loading data acquisition system with a capacity of 20 kN was installed on the loading frame, the same as a single granular pile. A group of 12 granular piles were installed in a triangular pattern. The diameter of the loading plate is selected in such a way that it inscribed the central three granular piles of the twelve granular pile group as suggested by (IS 15284 (part 1) 2003; Murugesan and Rajagopal 2010; Ghazavi and Nazari Afshar 2013; Ali et al. 2014).

For triangular pattern, the formula for area replacement ratio (A_r) as per (IS 15284 (part 1) 2003) is

$$A_r = 0.907\,(\frac{D}{s})^2 \tag{3.8}$$

Therefore, for A_r = 25% and diameter of granular pile (D) =60 mm, the spacing between granular piles (s) = 115 mm. The diameter of loading plate is determined as (D_p) = 194 mm, as shown in Fig. 3.24. Also, the loading plate was placed on top of the sand bed so that the center of the plate and load cell would coincide. The loading plate was adequately rigid, so there was no differential settlement during the tests. A comprehensive summary of the cyclic data retrieved from the stress-controlled data acquisition system for the group of granular piles has been plotted in Fig. 3.25, which illustrates the sinusoidal loading application, variation of q_{cy} with S_c, S_c with N, and q_{cy} with N up to 500 cycles.

Three PPTs were installed in the center of the test tank at a depth of 30 mm, 150 mm, and 270 mm from the loading plate level. P_{exc} data obtained from PPT installed in the middle of the test tank (i.e., 150 mm from the loading plate) are plotted in results and discussions, similar to the single granular pile. Similarly, two miniature pressure transducers (PT) (make KDE-200 kPa, KDE-1 MPa) were installed in the soil bed and surrounding granular pile at a depth of 30 mm to record stresses during loading. The pictorial view of PPTs and PTs is presented in Fig. 3.19, and their arrangement is shown in Fig. 3.26.The data from PPTs and PTs were recorded and retrieved from time to time using a DEWESOFT universal data acquisition system.

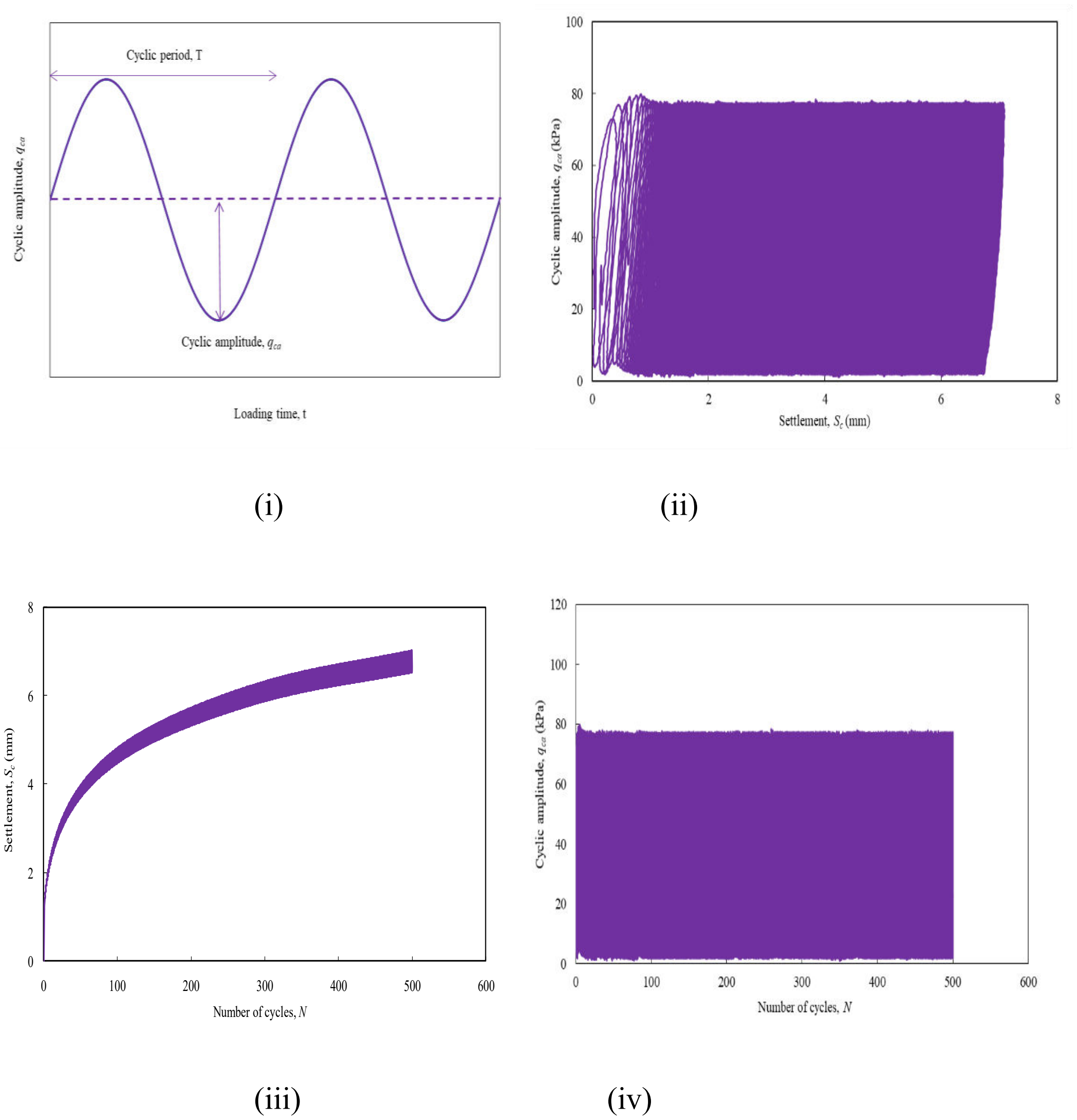

Fig. 3.25 (i) Schematic diagram of sinusoidal loading, (ii) variation of q_{cy} with S_c, (iii) variation of S_c with N, and (iv) variation of q_{cy} with N up to 500 number of cycles.

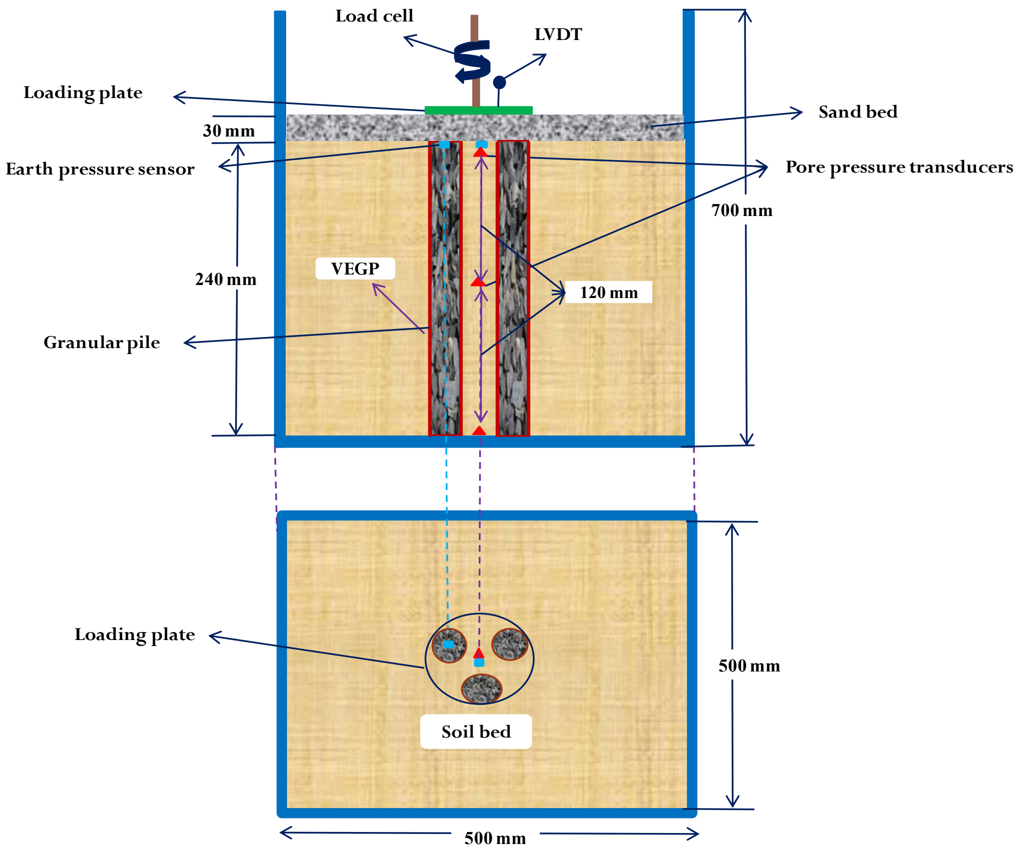

Fig. 3.26 A schematic sketch of the test set-up with earth pressure and pore pressure sensors.

The stress distribution at the model tank boundary walls was examined using earth pressure transducers installed near the tank boundaries. One EPT was placed on the soil bed at the boundary wall, and the other is on the outer most granular pile.The variation in stress distribution below the loading plate and at tank boundaries was recorded and represented in Fig. 3.27. In both cases, the in situ stresses measured were within permissible limits, i.e., less than 10%, as reported by (Ali et al., 2012), as outlined in Fig. 3.10(b).

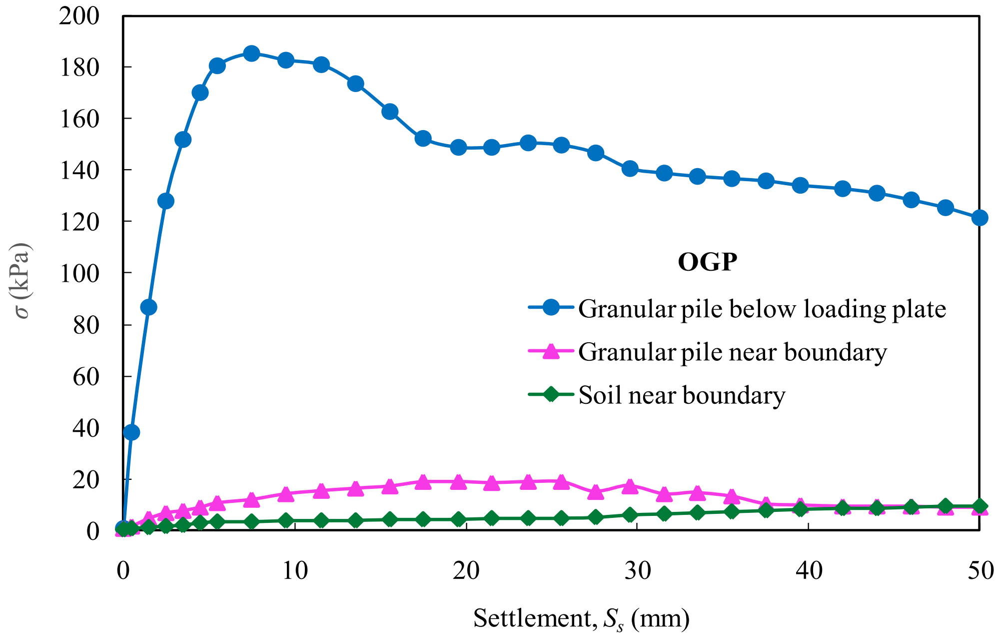

Fig. 3.27 The variation of stress distribution below the loading plate, and at tank boundaries using earth pressure transducers (EPTs).